RESEARCH ARTICLE

physica status solidi pss rrl
www.pss-rapid.com

Anomalous Response in the Orbital Magnetic Susceptibility of 2D Topological Systems

*Daniel Faílde and Daniel Baldomir**

2D compounds with nonzero Berry curvature are ideal systems to study exotic and technologically favorable thermoelectric and magnetoelectric properties. Within this class of materials, the topological trivial and nontrivial regimes have to present very different behaviors, which are encoded for the orbital susceptibility and magnetization. To try to reveal them, it is found that it was necessary to introduce a k-dependent mass term in the relativistic formalism of these materials. Thus, while a topologically trivial insulator is predicted to have a very limited response, in the nontrivial regime, a singular contribution to the orbital magnetic susceptibility, which is inversely proportional to the square of the quantum magnetic flux is unveiled. In this scenario, besides determining the measurement conditions a new route for enhancing the intrinsic orbital magnetism of topological materials widening the range of temperatures and magnetic fields without involving tiny bandgaps is found.

1. Introduction

The study of the thermoelectric and magnetoelectric properties in nonzero Berry curvature compounds has gathered great interest during the past years.[1–13] These advances are a consequence of the particular and favorable transport properties that these systems share and that have a direct implementation through graphene-like systems, topological insulators (TIs), Chern insulators (CIs), and Weyl semimetals.[14–20] Graphene-like systems are included because, despite not being necessarily topological, introducing terms such as a spin-orbit coupling and/or a staggered on-site potential in a honeycomb lattice we also have finite Berry curvatures.[21–24] For its part, TIs or CIs apply to a wider variety of structures and the dimensions of the space–time and the intrinsic symmetries of the system are essential elements.[25–27] Generally, most of the previous works focus on 2D materials, where the Abelian Berry curvature allows a simple determination of the system s topology by means of the first Chern number C.[28] In contrast, a generalization to higher dimensional systems is not immediate since this process involves dealing with non-Abelian terms in our calculations.[1,2]

Throughout different formalism, it has been shown how some properties of these systems such as the Berry curvature, density of states, orbital magnetic moment, and energy behave when applying a magnetic field.[4,7,9,10,12,13] The last effort provides analytical expressions to show how these magnitudes depend on the external magnetic field for a gapped Dirac spectrum.[12] Thus, it can be seen how an external magnetic field modulates the shape of the Berry curvature and the intrinsic orbital dynamics of the system. However, these calculations apply to any 2D nonzero Berry curvature material with a linear dispersion law while 2D and 3D TIs thin-films usually present non-negligible parabolic terms in their spectra.[16,17] To introduce such a term and study the orbital magnetization and susceptibility as well as other transport properties in an accurate way one needs to reach second-order corrections. This is done because some properties as the susceptibility or conductivities involve second derivatives in the energy with respect to the electromagnetic fields and the corrections become non-negligible at relatively low external fields due to the low energy nature of the relativistic models working on these materials.[9,12,13] In contrast, while an exact solution in terms of Landau levels can be achieved for a constant mass in an external magnetic field this method is likely to result tortuous when considering other interactions compared with the other specified formalisms.[29]

In this study, we introduce the role of the momentum-dependent mass term in the corrections to the Dirac Hamiltonian in presence of a magnetic field. Reaching second-order corrections to all the physical magnitudes involved, our calculations break the current scenario in which both inverted and normal band structures have an equivalent orbital magnetic response. In this line, we observe that the trivial insulator has a limited response to this parameter while a nontrivial insulator is predicted to show an anomalous response which can be written in terms of the square of the quantum magnetic flux. As an immediate consequence, it is shown how the intrinsic orbital magnetism of topologically non-trivial Berry curvature systems can be enhanced by increasing the parabolic dependence of their energy spectrum.

D. Faílde, D. Baldomir
Departamento de Física Aplicada
Instituto de Investigacións Tecnoloxicas
Universidade de Santiago de Compostela
Campus Vida s/n, Santiago de Compostela E-15782, Spain
E-mail: daniel.baldomir@usc.es

The ORCID identification number(s) for the author(s) of this article can be found under https://doi.org/10.1002/pssr.202200065.

DOI: 10.1002/pssr.202200065

2. Results

Our starting point is a solid-state version of the Dirac Hamiltonian used to describe 2D and 3DTIs[30]

$$H = M(\boldsymbol{k})\beta + v_F(\boldsymbol{\alpha} \times \boldsymbol{p}) \tag{1}$$

where the Fermi velocity v_F substitutes the speed of light c, $\beta = \sigma_z \otimes I_{2\times2}$ and $\alpha_i = \sigma_x \otimes \sigma_i$ are the Dirac matrices which are defined in terms of the Pauli matrices σ_i and the 2×2 identity matrix $I_{2\times2}$, $\boldsymbol{p} = \hbar\boldsymbol{k}$ the momentum of the particles and $M(k) = M - \mathcal{B}k^2$ a k-dependent diagonal term, where M and $\mathcal{B}$ depend directly on the on-site energies and second-neighbor hopping elements. This effective Hamiltonian allows a simple determination of the system s topology, especially on its 2D version, where we can easily differentiate between the topological nontrivial and trivial regimes by looking at the relative sign between the parameters M and $\mathcal{B}$. That is, it reduces to a Bernevig–Hughes–Zhang (BHZ) model with two noninteracting time-reversal copies $(M(k) \to -M(k))$ of a 2D Dirac Hamiltonian $H_{2D} = M(k)\sigma_z + v_F\boldsymbol{\sigma} \times \boldsymbol{p}$.[28,30] Thus, we have $M\mathcal{B} > 0$ for the nontrivial regime and $M\mathcal{B} < 0$ for the trivial one that fixes the integer Chern number C to be 1 or 0, respectively. Notice that $\mathcal{B}$ is usually negative as the energy tends to grow when increasing k and the energy spectrum of Equation (1) is given by $\xi = \pm\sqrt{(M - \mathcal{B}k^2)^2 + \hbar^2 v_F^2 k^2}$. So essentially the topology depends on the sign of M, which for the particular case $M < 0$ (inverted band structure) results in nontrivial. In **Figure 1**a we can find a representation of the energy spectra and spin-configuration of the bands of both nontrivial and trivial regimes in H_{2D}. For the full Hamiltonian Equation (1), Dirac hyperbolae shall be plotted twice to take into account spin degeneracy. A similar Hamiltonian can be obtained from a Kane–Mele model on a honeycomb lattice although with a different topological constraint for the $M\mathcal{B}$ parameters.[22]

Introducing a perpendicular magnetic field $\boldsymbol{B} = B\hat{\boldsymbol{z}}$ on H_{2D} causes a correction in the eigenstates of the systems that can be written as[9,12]

$$|n\rangle \to |n\rangle + \frac{eB}{(\xi^n - \xi^m)}\frac{1}{\hbar}(\partial_{k_y}\xi^m A_x^{mn} - \partial_{k_x}\xi^m A_y^{mn})|m\rangle \tag{2}$$

where $-e$ is the electron charge, $A_j^{mn} = i\langle m|\partial_{k_j} n\rangle$, $|n\rangle$ and $|m\rangle$ are the eigenstates of the bands n and m with energy ξ^n and ξ^m. These corrections represent the coupling effects between the magnetic field and Berry curvature of the bands, which induce corrections to the Berry potential, Berry curvature, particle s velocity, density of states, orbital magnetic moment, and energy.[12] Thus, for the Berry potential $\boldsymbol{A}^n = i\langle n|\partial_k n\rangle$ we find from Equation (2) that

$$A_j^n \to A_j^n + 2\mathrm{Re}\, A_j^{nm}\frac{\hbar\omega_z^n}{(\xi^n - \xi^m)} \tag{3}$$

being $\omega_z^n = \varepsilon_{zrs}\frac{eB_z}{\hbar}\frac{1}{\hbar}\partial_{k_r}\xi^m A_s^{mn}$.[9,12] These expressions involve quite tedious calculations especially if we want to take into account the role of the parameter $\mathcal{B}$ in our Hamiltonian or deal with a particle-hole antisymmetric system. We are going to focus on the first case given that as the current literature indicates, there are no differences in the orbital magnetic susceptibility at zero-field $\chi_{\mathrm{orb}}(B = 0)$ between the trivial and nontrivial regimes when we consider a gapped Dirac dispersion.[10,12,13,29,31] This is quite impressive given that both regimes present clear differences in their curvatures and χ_{orb} is directly related to it (Figure 1b). Remember that at zero temperature $\chi_{orb} = -\partial^2 E/\partial B^2$ being $E = \int \frac{dk}{(2\pi)^2} D\tilde{\xi}$ the density of energy, $D = 1 + \frac{eB\times\tilde{\Omega}}{\hbar}$ the modified density of states, $\tilde{\Omega}$ the modified Berry curvature and $\tilde{\xi} = \xi\left(1 - \frac{eB\cdot\Omega}{\hbar} + \mathcal{O}(B^2)\right)$ the corrected energy resulting from

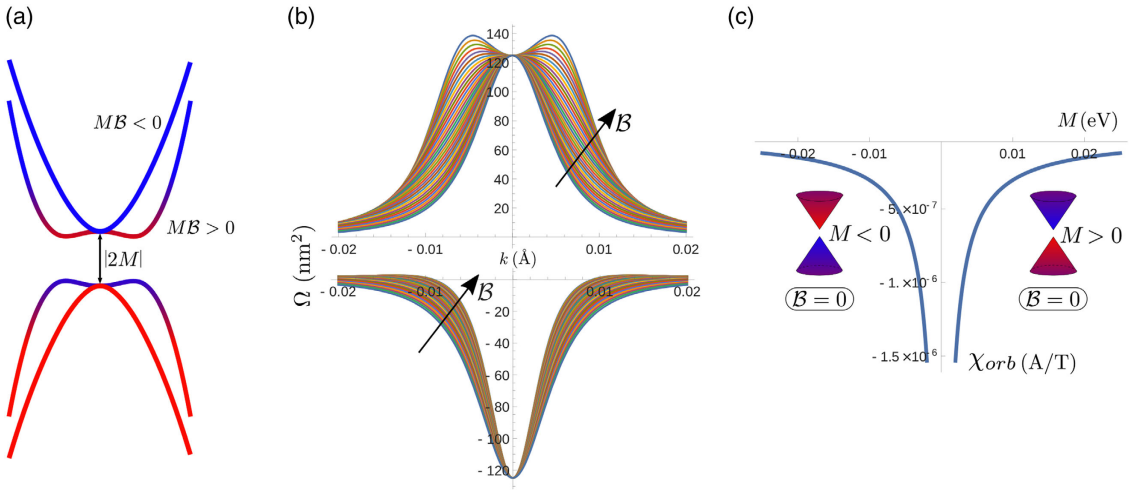

Figure 1. 2D features of low energy relativistic models. a) Energy spectra of a 2D Dirac Hamiltonian H_{2D} for the trivial ($M > 0$, $\mathcal{B} < 0$) and nontrivial ($M < 0$, $\mathcal{B} < 0$) cases. The color gradient indicates the z component of the k-dependent spin texture of each regime. In this configuration, the red color stands for spin down and blue for spin up, b) Berry curvature of the conduction band of H_{2D} for different values of $\mathcal{B}$ ranging from 0 to -300 eVÅ in steps of 10 eVÅ^2. The arrows indicate the change in Ω when increasing $\mathcal{B}$. c) Zero-field orbital magnetic susceptibility at $\mathcal{B} = 0$ (gapped Dirac dispersion) as a function of M.

the application of the magnetic field.[9] Then, one would expect to observe some differences although under linear dispersion conditions there are not (Figure 1c). Introducing $\mathcal{B}$ and after some algebra, it can be shown that the corrections of the Berry curvature $\boldsymbol{\Omega}^n = -2Im\langle \partial_{k_x} n | \partial_{k_y} n\rangle \hat{z} = \nabla \times \boldsymbol{A}$, obtained by applying Equation (2) or (3) to the eigenstates of H_{2D}, are given by

$$\tilde{\Omega} = \Omega + 2\frac{eB\Omega}{\hbar}\Omega\left(\frac{M-\mathcal{B}k^2}{(M+\mathcal{B}k^2)^2}F(k^2) - \frac{\hbar^2 v_F^2 k^2}{(M+\mathcal{B}k^2)^2}G(k^2)\right) \quad (4)$$

being $\xi = \pm\sqrt{(M-\mathcal{B}k^2)^2 + \hbar^2 v_F^2 k^2}$, $\Omega = -\hbar^2 v_F^2 (M+\mathcal{B}k^2)/(2\xi^3)$ and

$$F(k^2) = M - \frac{\xi^2 \mathcal{B}}{\hbar^2 v_F^2} - \frac{\mathcal{B}(M-\mathcal{B}k^2)(M+\mathcal{B}k^2)}{\hbar^2 v_F^2} \quad (5)$$

$$G(k^2) = 1 - 6\mathcal{B}\frac{M-\mathcal{B}k^2}{\hbar^2 v_F^2} + 6\mathcal{B}^2\frac{(M-\mathcal{B}k^2)^2}{\hbar^4 v_F^4} - 2\mathcal{B}^2\frac{\xi^2}{\hbar^4 v_F^4} \quad (6)$$

Equation (4–6) generalizes the results obtained for linear dispersions introducing $\mathcal{B}$, which is essential to define properly the Chern number $C = 1/(2\pi)\int \Omega d\boldsymbol{k}$ as an integer and distinguish the topological regime from the trivial one.[12,28] In fact, it can be tested numerically that the Chern number of the system is fixed for any given value as long as we maintain the sign of $M\mathcal{B}$ invariant.

Having $\tilde{\Omega}$ and hence D, we only need to calculate the second-order corrections for the energy induced by the perpendicular magnetic field B, which comes entirely from the coupling of the orbital magnetic moment of the electrons with the magnetic field in absence of Zeeman corrections.[9] Remember that the eigenstates corrections are obtained by introducing the magnetic field through the Peierls substitution in the Dirac Hamiltonian.[12] Then, the resulting perturbation ΔH to H_{2D} is not other than the product of the magnetic field and the orbital magnetic moment operator $\Delta H = \frac{eB}{2}(\hat{x}\hat{v}_y - \hat{y}\hat{v}_x) = -\hat{m}_z B$. This allows us to compute directly the elements $\langle n|\Delta H|n\rangle$ and $\langle n|\Delta H|m\rangle$ and obtain the energy corrections

$$\tilde{\xi} = \xi - mB + \frac{1}{2}\frac{(mB)^2}{\xi}\frac{\hbar^2 v_F^2 k^2}{(M+\mathcal{B}k^2)^2}\left(1 - 2\mathcal{B}\frac{(M-\mathcal{B}k^2)}{\hbar^2 v^2}\right)^2 \quad (7)$$

where $m = \frac{e}{\hbar}\xi\Omega$ is the orbital magnetic moment of the electrons in both conduction and valence bands of H_{2D}[28]. With these elements, it is straightforward to show how the orbital magnetization at zero-temperature $\mathcal{M}_{\text{orb}} = -\partial E/\partial B$ is a function of the magnetic field B given by $\mathcal{M}_{\text{orb}} = \mathcal{M}_1 B + \mathcal{M}_2 B^2 + \mathcal{M}_3 B^3$. Or equivalently, we have an orbital magnetic susceptibility $\chi_{orb} = \chi_0 + \chi_1 B + \chi_2 B^2$, where

$$\chi_0 = \frac{e^2 v_F^2(-1 + (1-2rs)\beta + 10(1+rs)\beta^2)}{6\pi(1-4\beta)M} \quad (8)$$

$$\chi_1 = -\frac{3e^3\hbar v_F^4}{64\pi M^3(1-4\beta)^{3/2}}\Lambda(\beta) \quad (9)$$

$$\chi_2 = \frac{e^4\hbar^2 v_F^6}{420\pi M^5(1-4\beta)^3}\Theta(\beta) \quad (10)$$

We defined $\beta = M\mathcal{B}/\hbar^2 v_F^2$, $s = sgn(M)$ and $r = sgn(\mathcal{B})$. A complete expansion of the functions $\Lambda(\beta)$ and $\Theta(\beta)$ can be found in the Supporting Information. Notice that χ_{orb} is given in units of amperes (A) per tesla (T) being typical to represent it as a dimensionless quantity by using a normalization parameter χ_n as the inverse of effective magnetic permeability μ in two dimensions. That is, $e^2 a v_F/(6\pi^2\hbar)$ for the particular case of a honeycomb lattice with lattice constant a.[10,13] In **Figure 2** we can see that χ_2 is practically paramagnetic for any value of M and $\mathcal{B}$, although a detailed inspection reveals a paramagnetic region defined by the condition $4M\mathcal{B} > \hbar^2 v_F^2$ ($\beta > 1/4$) for the nontrivial topological regime (Supporting Information). This term is liable to play an important role only for tiny gaps and/or high magnetic fields, where corrections due to Zeeman effects should also be considered. That is, for a typical gap $|2M| = 50\,\text{meV}$, $v_F = 6\times10^5\,\text{m s}^{-1}$, and a field $B = 1\text{T}$ whose equivalent energy ($\hbar\omega$) does not exceed this gap we have that $|\chi_2/\chi_0| \approx 10^{-3}$ and $|\chi_2/\chi_1| \approx 10^{-2}$. Attending to χ_1, its contribution to the orbital magnetization and susceptibility is opposite for both regimes resulting in paramagnetic for the topological nontrivial and diamagnetic for the normal state when B is positive. Compared to χ_0 the ratio between both is close to 10^{-1} under the same prior conditions and hence becomes to be non-negligible at relative low-magnetic fields depending on the band gap 2M of the system. Its dependence on $\mathcal{B}$ can be explored in more detail in the Supporting Information. Thus, besides it is evident that χ_2 and χ_1 have a weaker dependence on this parameter compared with M (Figure 2b,c), for a fixed gap both regimes show a very different response, with a nearly constant dependency for the trivial regime and strong for the topological one. Finally, note that for time-reversal symmetric systems such as Equation (1) in 2D the contribution of the two Chern species cancels each other and χ_1 will be zero while the even powers in the magnetic field for the susceptibility appear with a spin-degeneracy factor $g = 2$.

A significant result is obtained when analyzing the zero-field orbital susceptibility χ_0. A first look at Figure 2a indicates that there are clear differences with the current scenario in which χ_0 manifests the same behavior when considering gapped linear dispersions (Figure 1b). However, we can go further by subtracting the common background term at zero $\mathcal{B}$ displayed in Figure 1c from Equation (8). This factor is obtained by different methods and it is equal to $\chi_M = -\frac{e^2 v^2}{6\pi|M|}$.[10,12,13,29,31] In this way, we find that it appears a continuum spectrum for $\chi_0 - \chi_M$ with a ratio $\frac{5}{6\pi}\frac{e^2}{\hbar^2}$ given in fundamental units when plotted versus $\mathcal{B}$ (**Figure 3**). This unexpected behavior belongs uniquely to the topological regime while for the trivial we have a non-homogeneous dependence on $\mathcal{B}$. In general formulae, we can write the zero-orbital magnetic susceptibility for both topological and nontrivial

$$\chi_0 = -\frac{e^2 v^2}{6\pi|M|} + \frac{5e^2}{6\pi\hbar^2}\mathcal{B} \qquad (M<0, \mathcal{B}<0) \quad (11)$$

and trivial phases

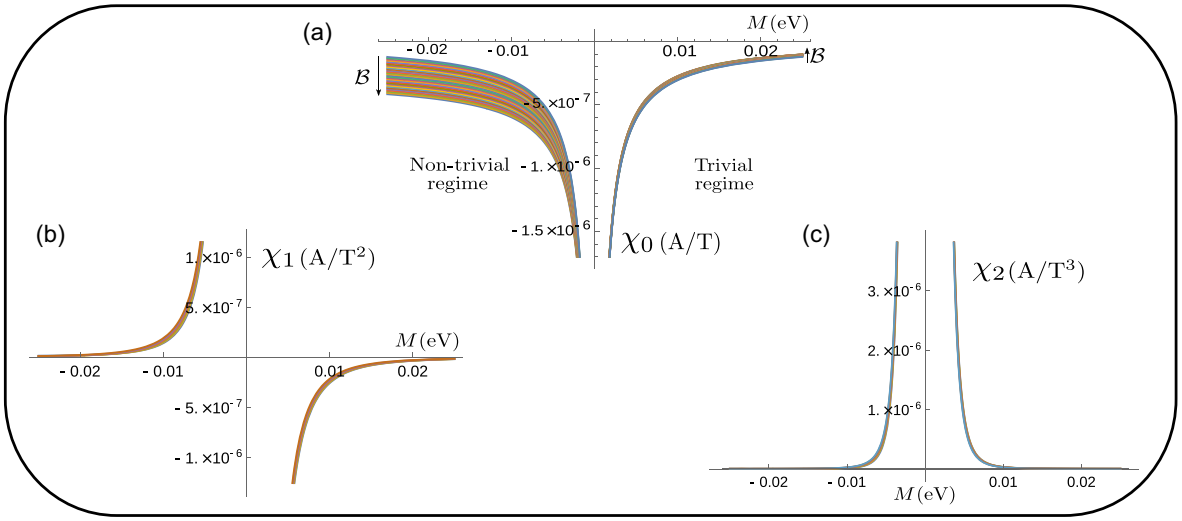

Figure 2. Orbital magnetic susceptibility in non-zero Berry curvature systems. a) Zero-field orbital magnetic susceptibility of the trivial and nontrivial topological regimes. $\mathcal{B}$ ranges from 0 to $-300\,\text{eVÅ}^2$ and v_F is set to $6\times10^5\,\text{m s}^{-1}$. In contrast to the current scenario displayed in Figure 1c, the introduction of the parabolic dependence at large k given by $\mathcal{B}$ determines a drastic change in the behavior of both regimes: b,c) Linear (χ_1) and quadratic (χ_2) coefficients in the magnetic field of the orbital susceptibility.

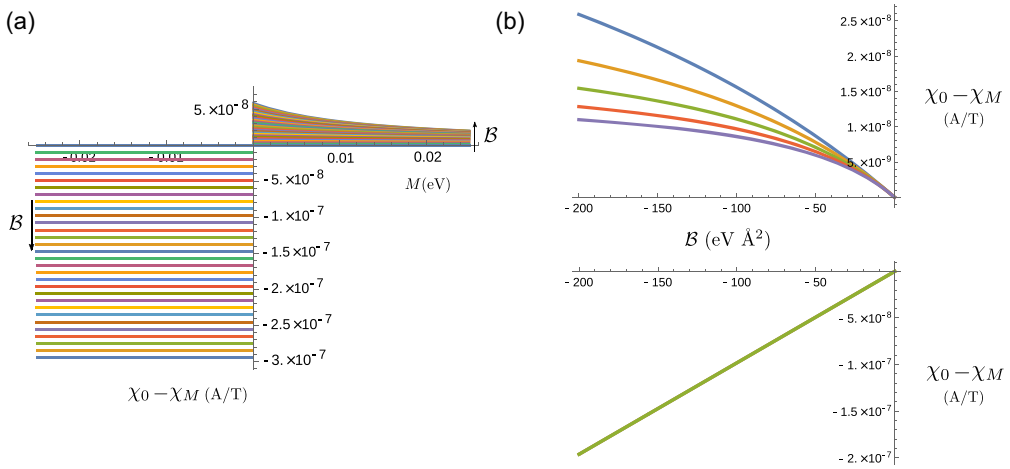

Figure 3. Normalized zero-field orbital magnetic susceptibility. a) $\chi_0-\chi_M$ versus M for different $\mathcal{B}\in[-300,0]$ eVÅ^2. b) $\chi_0-\chi_M$ versus $\mathcal{B}$ for different values of M ranging from 10 (blue line) to 50 meV (purple line). The upper panel represents the behavior of the normalized zero-orbital susceptibility in a trivial insulator $M\mathcal{B}<0$ whereas the lower panel stands for a topologically nontrivial insulator ($M\mathcal{B}>0$). This latter case exhibits no dependence on the gap giving a linear diamagnetic contribution to the zero-orbital susceptibility.

$$\chi_0=-\frac{e^2v^2(\hbar^2v_F^2-3M\mathcal{B})}{6\pi|M|(\hbar^2v_F^2-4M\mathcal{B})}\qquad(M>0,\mathcal{B}<0)\tag{12}$$

$$\mu\chi_0\propto -C_1\frac{t_1}{|\xi_\nu-4t_2|}-C_2\frac{t_2}{t_1}\tag{13}$$

by introducing in the same expression the principal parameters M, $\mathcal{B}$, and v_F for the topology and transport which are directly related to the different hopping elements. Thus, roughly speaking for the simplest case of a square lattice with complex spin-dependent first-neighbor hopping it_1 and staggering potential for the on-site energies ξ_ν and second-neighbor hopping t_2 we can reach for the topological regime that

obtaining from the tight-binding that $v_F=2at_1/\hbar$, $M=\xi_\nu-4t_2$, $\mathcal{B}=-2t_2a^2$, $\mu^{-1}\propto e^2v_Fa/\hbar$. Numerical factors accompanying these relations will depend on the crystal structure of the system which determines the coefficients C_1 and C_2.

We can also observe by computing the large $\mathcal{B}$ limit ($M\mathcal{B}>>\hbar^2v_F^2$) that χ_0 grows linearly for the topological regime while it saturates in a finite value $-\frac{e^2v^2}{8\pi M}$ ($M>0$) for the trivial insulator with a softer dependence on this parameter (Figure 3b). The role of $\mathcal{B}$ opens a new possibility for tuning

the orbital magnetization and susceptibility in topological materials breaking the current scenario in which we need to employ materials with a tiny gap for maximizing the response. This could be experimentally unpleasant given that then you are limited to working with a small frame of temperature and/or magnetic fields. Notice that the orbital susceptibility, also known as geometrical, is dominant only inside the bandgap and decays to zero as the Fermi level enters the conduction and valence bands.[10] In other words, a more robust parabolic dependence in the energy spectra causes an enhanced orbital magnetic response in topological materials.

The present results have another direct experimental consequence. In contrast, directly from Equation (12), it is straightforward to note that the dependence on $\mathcal{B}$ in the trivial regime seems to be weak, as one can verify it by computing the ratio $(\hbar^2 v_F^2 - 3M\mathcal{B})/(\hbar^2 v_F^2 - 4M\mathcal{B})$ under the high Fermi velocity and small gap conditions that these systems feature. Typically, these are in the range of $10^5 - 10^6\,\mathrm{m\,s^{-1}}$ for the velocity while the gap is in the order of meV.[17,30,32] In contrast, a topological nontrivial insulator shows a ratio $\propto \frac{e^2}{\pi\hbar^2}$ independent of such parameters which can be related directly to the quantum magnetic flux $\Phi_0 = h/(2e)$. Thus, varying $\mathcal{B}$ we expect a change in the orbital magnetic susceptibility $\Delta\chi_0 \propto \pi/\Phi_0^2$. This result seems to connect perfectly with the concept of orbit for the topological electrons developed in 2D and 3DTI thin films by translating the topological information contained in the Berry curvature into a topological effective field b.[11] In this theory, the topological quantization through C and the low energy nature of the topological electrons are employed to associate a quantized flux to each orbit and determine an effective magnetic field b and area ΔS for these electrons

$$b \approx \frac{(2)m^2 v_F^2}{\hbar e} \qquad \Delta S \approx \frac{h\hbar}{(2)m^2 v_F^2} \tag{14}$$

Here m is the effective mass and factor (2) vanishes when redefining the orbital magnetic moment.[12] That is, matching b with the solid-state version of the Schwinger critical field.[33] In summary, it can be defined as a magnetic field b from the Berry curvature on each band of a TI or Chern insulator with a net value of zero in presence of time-reversal symmetry. Physically, it is straightforward to connect these results with the ones obtained for the orbital magnetic susceptibility. Looking at the energy dispersion it is obvious that varying $\mathcal{B}$ makes it more localized/delocalized in the k-space and modifies the effective mass m of the particles. Therefore, as long as the topology is the same ($sgn(M\mathcal{B})$ remains invariant), this will just change the effective area of the electrons ΔS and also the field b associated with each band but keeping its flux invariant. This will redefine the orbit, its related properties (Berry curvature, energy, particle s velocity...) and also the orbital magnetic response of the system. However, given that this maintains the same quantized nature, it is expectable to get an orbital magnetic susceptibility which grows with this flux and also no variations in the topological trivial regime due to the absence of orbits associated to their trivial Berry curvatures ($C = 0$).

Further corrections can be taken into account implying that the numerical factor accompanying π/Φ_0^2 in the second term of Equation (11) should experiment changes. Notice that by considering $\mathcal{B}$ in our Hamiltonian we are introducing a k-dependent mass term in our system. So the perpendicular magnetic field should also give a diagonal contribution to the perturbed Hamiltonian that could be introduced in Equation (2). This would lead to more accurate expressions but from the physical point of view, this would also imply the necessity to consider Zeeman corrections. Nevertheless, if one performs the simple calculation associated with first-order corrections of this term to the energy it is easy to show that $\langle n|\Delta H_z|n\rangle = \frac{eB}{2\hbar}\mathcal{B}$ being $\Delta H_z = \frac{eB}{\hbar}\mathcal{B}\sigma_z(k_x y - k_y x)$. Comparing this factor with the first-order term $-m \times B$, we can verify that at low energy $\frac{eB\mathcal{B}/\hbar}{eB\xi\Omega/\hbar} \approx \frac{M\mathcal{B}}{\hbar^2 v^2}$ is again negligible for a wide range of parameters that typically characterize these materials.

3. Conclusion

All materials respond as paramagnetic or diamagnetic under an applied external magnetic field although their physical origins are very different. For example, diamagnetism depends mainly on the atomic number and the orbital electron radius, while paramagnetism strongly depends on the temperature and magnetic momenta of the ground state within the first-order approach. This last condition can be overcome by introducing higher order perturbative terms as occurs with van Vleck paramagnetism when also considering the magnetization of excited states. However, in 2D materials with nonzero Berry curvature, new orbital magnetizations emerge from this property. In this context, as we show in Figure 2 and 3, we found new terms in the orbital magnetic susceptibility of the topological nontrivial regime which is susceptible to be measured and open a new form to modulate the intrinsic orbital magnetism of topological materials.

Concretely, we theoretically analyzed the orbital dynamics of 2D nonzero Berry curvature systems by introducing the natural k dependence in the energy dispersion and mass that the Dirac electrons have in condensed matter. Given the crucial role of this term for a proper definition of the topological invariant Chern number, the analytical expressions which result from this perturbative analysis of the Dirac Hamiltonian in presence of a perpendicular magnetic field are able to disentangle the topological orbital effects besides extending the previous results using linear dispersion to a broader variety of compounds. The new scenario which arises involves drastic differences in the orbital magnetic response of the topological trivial and nontrivial regimes. Thus, while a trivial insulator is predicted to have a limited dependence on $\mathcal{B}$ based on the common values that these materials have, its topological counterpart features an unexplored term in the zero-field orbital magnetic susceptibility which is given in fundamental units and is inversely proportional to the square of the quantum magnetic flux. The results obtained go further in the study of singular physics of these materials approaching it to the quantum phase transition phenomenology and enabling different paths to modulate the orbital magnetization and susceptibility in these materials. As well, they establish the basis to treat directly other nonlinear

thermoelectric and magnetoelectric properties of nonzero Berry curvature systems.

Supporting Information

Supporting Information is available from the Wiley Online Library or from the author.

Acknowledgements

The authors acknowledge PID2019-104150RB-I00, AEMAT ED431E 2018/08 and the MAT2016-80762-R projects for financial support. The authors thank Juan Manuel Faílde for the helpful discussions. The authors acknowledge CESGA for computational facilities.

Conflict of Interest

The authors declare no conflict of interest.

Data Availability Statement

The data that support the findings of this study are available from the corresponding author upon reasonable request.

Keywords

Berry curvature, orbital susceptibility, topological insulators

Received: February 18, 2022
Revised: May 30, 2022
Published online: June 28, 2022

[1] X.-L. Qi, T. L. Hughes, S.-C. Zhang, *Phys. Rev. B* **2008**, *78*, 195424.
[2] D. Baldomir, D. Faílde, *Sci. Rep.* **2019**, *9* 6324.
[3] D. Xiao, M.-C. Chang, Q. Niu, *Rev. Mod. Phys.* **2010**, *82*, 1959.
[4] D. Xiao, J. Shi, Q. Niu, *Phys. Rev. Lett.* **2005**, *95*, 137204.
[5] T. Thonhauser, D. Ceresoli, D. Vanderbilt, R. Resta, *Phys. Rev. Lett.* **2005**, *95*, 137205.
[6] D. Xiao, Y. Yao, Z. Fang, Q. Niu, *Phys. Rev. Lett.* **2006**, *97*, 026603.
[7] J. Shi, G. Vignale, D. Xiao, Q. Niu, *Phys. Rev. Lett.* **2007**, *99*, 197202.
[8] T. Qin, Q. Niu, J. Shi, *Phys. Rev. Lett.* **2011**, *107*, 236601.
[9] Y. Gao, S. A. Yang, Q. Niu, *Phys. Rev. Lett.* **2014**, *112*, 166601.
[10] Y. Gao, S. A. Yang, Q. Niu, *Phys. Rev. B* **2015**, *91*, 214405.
[11] D. Faílde, D. Baldomir, *Sci. Rep.* **2021**, *11*, 14335.
[12] D. Faílde, D. Baldomir, *New J. Phys.* **2021**, *23*, 113002.
[13] S. Ozaki, M. Ogata, *Phys. Rev. Res.* **2021**, *3*, 013058.
[14] G. R. Bhimanapati, Z. Lin, V. Meunier, Y. Jung, J. Cha, S. Das, D. Xiao, Y. Son, M. S. Strano, V. R. Cooper, L. Liang, S. G. Louie, E. Ringe, W. Zhou, S. S. Kim, R. R. Naik, B. G. Sumpter, H. Terrones, F. Xia, Y. Wang, J. Zhu, D. Akinwande, N. Alem, J. A. Schuller, R. E. Schaak, M. Terrones, J. A. Robinson, *ACS Nano* **2015**, *9*, 11509.
[15] Q. Liu, X. Zhang, L. B. Abdalla, A. Fazzio, A. Zunger, *Nano Lett.* **2015**, *15*, 1222.
[16] M. König, S. Wiedmann, C. Brüne, A. Roth, H. Buhmann, L. W. Molenkamp, X.-L. Qi, S.-C. Zhang, *Science* **2007**, *318*, 766.
[17] H. Zhang, C.-X. Liu, X.-L. Qi, X. Dai, Z. Fang, S.-C. Zhang, *Nat. Phys.* **2009**, *5*, 438.
[18] J. Li, Y. Li, S. Du, Z. Wang, B.-L. Gu, S.-C. Zhang, K. He, W. Duan, Y. Xu, *Sci. Adv.* **2019**, *5*, 6.
[19] Y. Deng, Y. Yu, M. Z. Shi, Z. Guo, Z. Xu, J. Wang, X. H. Chen, Y. Zhang, *Science* **2020**, *367*, 895.
[20] Y. Xue, B. Zhao, Y. Zhu, T. Zhou, J. Zhang, N. Li, H. Jiang, Z. Yang, *NPG Asia Mater.* **2018**, *10*, e467.
[21] C. L. Kane, E. J. Mele, *Phys. Rev. Lett.* **2005**, *95*, 146802.
[22] C. L. Kane, E. J. Mele, *Phys. Rev. Lett.* **2005**, *95*, 226801.
[23] D. N. Sheng, Z. Y. Weng, L. Sheng, F. D. M. Haldane, *Phys. Rev. Lett.* **2006**, *97*, 036808.
[24] M. Schüler, U. D. Giovannini, H. Hübener, A. Rubio, M. A. Sentef, P. Werner, *Sci. Adv.* **2020**, *6*, eaay2730.
[25] J. E. Moore, L. Balents, *Phys. Rev. B* **2007**, *75*, 121306.
[26] L. Fu, C. L. Kane, *Phys. Rev. B* **2007**, *76*, 045302.
[27] A. P. Schnyder, S. Ryu, A. Furusaki, A. W. W. Ludwig, *Phys. Rev. B* **2008**, *78*, 195125.
[28] H.-Z. Lu, W.-Y. Shan, W. Yao, Q. Niu, S.-Q. Shen, *Phys. Rev. B* **2010**, *81*, 115407.
[29] M. Koshino, T. Ando, *Phys. Rev. B* **2010**, *81*, 195431.
[30] B. A. Bernevig, T. L. Hughes, S.-C. Zhang, *Science* **2006**, *314*, 1757.
[31] H. Fukuyama, *J. Phys. Soc. Jpn.* **2007**, *76*, 043711.
[32] D. C. Elias, R. V. Gorbachev, A. S. Mayorov, S. V. Morozov, A. A. Zhukov, P. Blake, L. A. Ponomarenko, I. V. Grigorieva, K. S. Novoselov, F. Guinea, A. K. Geim, *Nat. Phys.* **2011**, *7*, 701.
[33] G. V. Dunne, C. Schubert, *Phys. Rev. D* **2005**, *72*, 105004.